Asymptotic solutions for an electrically induced Freedericksz transition in a wedge of smectic C liquid crystal

2006 J. Phys. A: Math. Gen. 39 11361

(http://iopscience.iop.org/0305-4470/39/37/003)

INSTITUTE OF PHYSICS PUBLISHING JOURNAL OF PHYSICS A: MATHEMATICAL AND GENERAL

J. Phys. A: Math. Gen. **39** (2006) 11361–11382 doi:10.1088/0305-4470/39/37/003

Asymptotic solutions for an electrically induced Freedericksz transition in a wedge of smectic C liquid crystal

A A T Smith[1] **and I W Stewart**[2]

[1] School of Biomedical and Natural Sciences, Nottingham Trent University, Erasmus Darwin Building, Clifton Lane, Clifton, Nottingham, NG11 8NS, UK
[2] Department of Mathematics, University of Strathclyde, Livingstone Tower, 26 Richmond Street, Glasgow, G1 1XH, UK

E-mail: andrew.smith@ntu.ac.uk and i.w.stewart@strath.ac.uk

Received 21 April 2006, in final form 4 July 2006
Published 29 August 2006
Online at stacks.iop.org/JPhysA/39/11361

Abstract

Theoretical work based on the Freedericksz transition in a wedge of smectic C liquid crystal is presented. Continuum theory is employed in order to mathematically model the two-way interaction between the anisotropic fluid and an applied electric field. Asymptotic methods are used to obtain concise and informative explicit solutions for limiting regimes where (a) the applied voltage is just above threshold, and (b) a high voltage is applied. As is anticipated, in the case of a small dielectric anisotropy, the solution reduces to that obtained when the two-way interaction is neglected. Nevertheless, at voltages close to threshold, this interaction can have a significant effect upon the director profile. Realistic material, geometry and field parameters are adopted in order to display these solutions. By comparing them with those obtained using a numerical method, a high degree of accuracy can be found within the above regimes.

PACS numbers: 61.30.−v, 61.30.Dk

1. Introduction

Liquid crystals are anisotropic fluids which often consist of rod-like molecules. The unit vector **n**, commonly called the director, indicates the average alignment of the molecular axes and it is usually sufficient for a description of what are referred to as nematic liquid crystals in the isothermal state. When applying an electric or magnetic field to a sample of liquid crystal the director will often reorient in order to align with the field. Depending on the sign of the dielectric or magnetic anisotropy, the director will either try to align parallel or perpendicular to the field. For the special case when the dielectric or magnetic anisotropy is positive and the

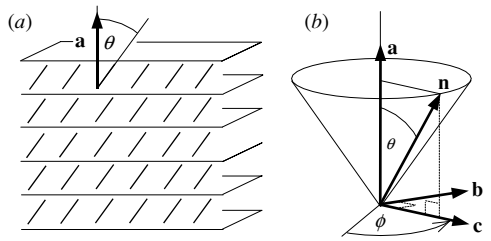

Figure 1. (*a*) The local alignment of the director, represented by short bold lines, arranged in equidistant layers of SmC liquid crystal. The director makes a constant tilt angle θ with respect to the smectic layer normal **a**. (*b*) The geometrical description of SmC. The director **n** can rotate around the surface of a fictitious cone as indicated. The vector **c** is the unit orthogonal projection of **n** onto the smectic planes and **b** is defined by $\mathbf{b} = \mathbf{a} \times \mathbf{c}$. The orientation of **n** can be deduced from the orientation angle ϕ, defined relative to some fixed axis, for the vector **c** within the smectic planes as shown.

director is initially perpendicular to the field, it is found that alignment will only start to occur once a certain threshold field (the Freedericksz threshold) is reached (a similar scenario occurs when the dielectric or magnetic anisotropy is negative and the director is initially aligned parallel to the field). The theory behind this phenomenon can be found in the texts by de Gennes and Prost [1] or Stewart [2]. Smectic C (SmC) liquid crystals consist of parallel layers of molecules where the director is tilted by an angle θ, called the smectic tilt or cone angle, relative to the local layer normal **a** and is forced to lie on the surface of a fictitious cone as shown in figure 1 [1, 2]. It proves mathematically convenient to introduce the vector **c** as the unit orthogonal projection of **n** onto the smectic planes and define the vector $\mathbf{b} = \mathbf{a} \times \mathbf{c}$. The orientation of **n** can be deduced from the orientation angle ϕ for the vector **c** within the smectic planes as shown in figure 1(*b*). Recent work in the literature has focused on various feasible SmC geometries. Rapini [3], in the context of the continuum theory developed by the Orsay Group [4], investigated Freedericksz transitions in planar configurations. The later theory proposed by Leslie *et al* [5, 6] then paved the way for further research into various geometries, as has been investigated by, among others, Carlsson *et al* [7], Atkin and Stewart [8, 9, 10], Kedney and Stewart [11], Barratt and Duffy [12] and Kidd *et al* [13]. Related work on the Freedericksz transition in planar SmC samples has also been carried out by Pelzl *et al* [14]. The developments described in this present paper are particularly motivated by the earlier results for Freedericksz transitions in a wedge of SmC [7, 9, 10] and it is the aim here to extend these analyses in order to incorporate more realistic electric field phenomena.

It is frequently assumed that an electric field is not influenced by the liquid crystal during the Freedericksz transition and that it is uniform over the sample. However, it is known that such an approximation to the field does not generally reflect the physical situation since the field and the liquid crystal interact with each other. Deuling [15], and later Welford and Sambles [16], looked at this problem in a planar nematic liquid crystal cell and found that significant effects on the distortion configuration occurred when the field is not assumed to be uniformly distributed across the sample. It is the intention here to include the electric field interaction with the liquid crystal in order to better model the Freedericksz effect in a wedge of SmC liquid crystal.

The current authors have shown previously [17] that it is possible to obtain an accurate description of the static behaviour in such a sample by solving a complex system of integral equations. Unfortunately, this complexity obscures the problem slightly, making it difficult to pick out the important governing parameters: it also forces the use of elaborate numerical

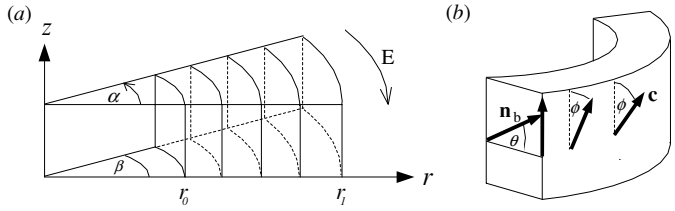

Figure 2. (*a*) The wedge geometry for SmC in the usual r, α and z cylindrical polar coordinate system. The boundary plates are located at $\alpha = 0$ and $\alpha = \beta$ and an electric field is applied across the plates. The cylindrically aligned SmC layers are arranged as shown in the region where $0 < r_0 \leqslant r \leqslant r_1$ and $0 \leqslant \alpha \leqslant \beta$. (*b*) A schematic representation of one cylindrical layer in the wedge. The fixed orientation of the director on the boundaries is denoted by $\mathbf{n}_b$ and the orientation angle ϕ of the vector $\mathbf{c}$ is defined in the local $z\alpha$-plane as shown.

methods. It is therefore desirable, in these circumstances, to use some asymptotic methods in order to look at different cases where certain terms can be neglected in order to gain some insight into the key influential mathematical or physical parameters. Schiller [18] has used a perturbation method in order to derive simpler approximate analytical solutions for a twisted nematic cell when the deformation is small and, more recently, Self *et al* [19] utilized asymptotic expansions to analytically investigate and extend the previous work of Deuling [15] for a planar nematic cell. Guided by the latter, we obtain analogous approximations for the Freedericksz transition in the SmC wedge, thereby extending the work of Carlsson *et al* [7] and Atkin and Stewart [9], yet simplifying the complex nature of a previous solution [17]. Further information on the asymptotic methods used below can be found in the book by Van Dyke [20].

The basic model of the wedge geometry for SmC and the governing differential equations are introduced in section 2 where the key non-dimensionalized equations are given by (2.18), (2.19) and (2.21). These equations form the basis for subsequent sections. The effect of small dielectric anisotropy is discussed in section 3 before going on to examine the low and high voltage cases (relative to the critical threshold voltage) in sections 4 and 5, respectively. The paper ends with a short discussion in section 6.

2. Model and governing equations

The wedge geometry for SmC liquid crystals [7, 9, 10, 21, 22] is known to be a resourceful research vehicle for determining properties of liquid crystals that are relevant to display and other technologies. It consists of placing a liquid crystal material between two angled plates across which a voltage is applied so as to obtain an azimuthal field. This configuration is shown in figure 2 where β denotes the wedge angle, $\mathbf{n}_b$ is the fixed director orientation at the boundaries, $\mathbf{E}$ is the electric field and r, α and z define the usual polar coordinate system.

When the applied field exceeds the Freedericksz threshold the director $\mathbf{n}$ will rotate around a fictitious cone. Figure 2(*b*) depicts a schematic view of one typical cylindrical layer in the wedge and shows the possible orientation of $\mathbf{c}$ as its orientation angle ϕ, as depicted in the figure, varies with α. We shall suppose that ϕ is a function of α only, i.e., $\phi = \phi(\alpha)$, since, by the geometry of the problem [7], it can be assumed that there is no dependence upon z or r. Following Carlsson *et al* [7], strong anchoring will be imposed on the director at the boundary plates so that

$$\mathbf{n}_b = \widehat{\mathbf{r}}\cos\theta + \widehat{\mathbf{z}}\sin\theta, \qquad \text{at} \quad \alpha = 0, \beta, \tag{2.1}$$

are the fixed director positions on the boundary plates. Note that if no field is present and strong anchoring given by (2.1) holds then there will be an unperturbed configuration corresponding to the constant solution $\mathbf{n} \equiv \mathbf{n}_b$.

The vectors $\mathbf{a}$ and $\mathbf{c}$ are subject to the constraints

$$\mathbf{a}\cdot\mathbf{a} = 1, \qquad \mathbf{c}\cdot\mathbf{c} = 1, \qquad \mathbf{a}\cdot\mathbf{c} = 0. \tag{2.2}$$

Oseen [23] observed that $\nabla \times \mathbf{a} = \mathbf{0}$, for smectic materials and this constraint has since been widely employed, especially by the Orsay Group [4] for planar layers of SmC. This constraint is valid for any lamellar-type system free from any defects or singularities and it will be supposed here also. Under the conditions (2.2) and the Oseen constraint it is now possible to write the following ansatz for $\mathbf{a}$, $\mathbf{b}$ and $\mathbf{c}$ [7]:

$$\mathbf{a} = \widehat{\mathbf{r}}, \qquad \mathbf{b} = -\widehat{\boldsymbol{\alpha}}\cos\phi + \widehat{\mathbf{z}}\sin\phi, \qquad \mathbf{c} = \widehat{\boldsymbol{\alpha}}\sin\phi + \widehat{\mathbf{z}}\cos\phi. \tag{2.3}$$

It is evident from the geometry of figure 2(b) that the strong anchoring conditions (2.1) lead to the boundary conditions

$$\phi(0) = \phi(\beta) = 0, \tag{2.4}$$

on ϕ and that the director can be described as [7]

$$\mathbf{n} = \mathbf{a}\cos\theta + \mathbf{c}\sin\theta = \widehat{\mathbf{r}}\cos\theta + \widehat{\boldsymbol{\alpha}}\sin\theta\sin\phi + \widehat{\mathbf{z}}\sin\theta\cos\phi. \tag{2.5}$$

Note that when $\mathbf{a}$ and θ are fixed, as they will be here, knowledge of ϕ gives a complete description for the orientation of director $\mathbf{n}$ via (2.5).

In order to perform an asymptotic analysis, differential equations governing the director orientation and field behaviour must be obtained by minimizing the total energy involved in the liquid crystal sample depicted in figure 2(a). It is known that the SmC elastic energy density can be written as [6]

$$\begin{aligned} w_C = {} & \tfrac{1}{2}A_{12}(\mathbf{b}\cdot\nabla\times\mathbf{c})^2 + \tfrac{1}{2}A_{21}(\mathbf{c}\cdot\nabla\times\mathbf{b})^2 + A_{11}(\mathbf{b}\cdot\nabla\times\mathbf{c})(\mathbf{c}\cdot\nabla\times\mathbf{b}) + \tfrac{1}{2}B_1(\nabla\cdot\mathbf{b})^2 \\ & + \tfrac{1}{2}B_2(\nabla\cdot\mathbf{c})^2 + \tfrac{1}{2}B_3\left[\tfrac{1}{2}(\mathbf{b}\cdot\nabla\times\mathbf{b} + \mathbf{c}\cdot\nabla\times\mathbf{c})\right]^2 \\ & + B_{13}(\nabla\cdot\mathbf{b})\left[\tfrac{1}{2}(\mathbf{b}\cdot\nabla\times\mathbf{b} + \mathbf{c}\cdot\nabla\times\mathbf{c})\right] \\ & + C_1(\nabla\cdot\mathbf{c})(\mathbf{b}\cdot\nabla\times\mathbf{c}) + C_2(\nabla\cdot\mathbf{c})(\mathbf{c}\cdot\nabla\times\mathbf{b}), \end{aligned} \tag{2.6}$$

where A_i, B_i and C_i represent elastic constants used by the Orsay Group [4] with the exception that $A_{11} = -\frac{1}{2}A_{11}^{\text{Orsay}}$ and $C_1 = -C_1^{\text{Orsay}}$. By substituting equations (2.3) into w_C, it is found that the total elastic energy in a wedge of SmC liquid crystal occupying a region of unit height in z with $0 < r_0 \leqslant r \leqslant r_1$ and $0 \leqslant \alpha \leqslant \beta$ is given by

$$\begin{aligned} W_C &= \iiint_V w_C r \,\mathrm{d}r\,\mathrm{d}\alpha\,\mathrm{d}z \\ &= \frac{1}{2}\ln\left(\frac{r_1}{r_0}\right)\int_0^\beta \Bigg[-A_{11} + [(A_{12}+A_{11})\sin^4\phi + (A_{21}+A_{11})\cos^4\phi] \\ &\quad + \left(\frac{\mathrm{d}\phi}{\mathrm{d}\alpha}\right)^2 [B_1\sin^2\phi + B_2\cos^2\phi] + 2\frac{\mathrm{d}\phi}{\mathrm{d}\alpha}[C_1\sin^2\phi - C_2\cos^2\phi]\cos\phi \Bigg]\mathrm{d}\alpha. \end{aligned} \tag{2.7}$$

The application of an electric field to a sample of SmC material induces an electric displacement $\mathbf{D}$ which can be directly related to the director $\mathbf{n}$ via [2, p 27]

$$\mathbf{D} = \epsilon_0\epsilon_\perp\mathbf{E} + \epsilon_0\epsilon_a(\mathbf{n}\cdot\mathbf{E})\mathbf{n}, \qquad \epsilon_a = \epsilon_\parallel - \epsilon_\perp, \tag{2.8}$$

where the constant ϵ_0 is the permittivity of free space, $\epsilon_\parallel$ and $\epsilon_\perp$ denote the relative dielectric

permittivities of the liquid crystal parallel and perpendicular to the director, respectively, and ϵ_a represents the unitless dielectric anisotropy of the SmC material. It should be noted, however, that this expression is only valid when the biaxiality of the material is small. Jones and Raynes [24] have made measurements of the biaxial permittivities for several SmC materials and it was seen that this assumption is often valid close to the SmC→SmA transition temperature. The electric energy density is given by [2, p 28]

$$w_{\text{elec}} = -\tfrac{1}{2}\mathbf{D}\cdot\mathbf{E} = -\tfrac{1}{2}\epsilon_0\epsilon_\perp E^2 - \tfrac{1}{2}\epsilon_0\epsilon_a(\mathbf{n}\cdot\mathbf{E})^2, \tag{2.9}$$

where $E = |\mathbf{E}|$. From standard electrostatic theory it is known that the electric field can be related to the electric potential Ψ via the relation $\mathbf{E} = -\nabla\Psi$ [25, p 47] where, to obtain the correct form for $\mathbf{E}$, it is expected that $\Psi = \Psi(\alpha)$ so that

$$\mathbf{E} = -\frac{1}{r}\frac{\mathrm{d}\Psi}{\mathrm{d}\alpha}\widehat{\boldsymbol{\alpha}}. \tag{2.10}$$

Inserting equations (2.5) and (2.10) into the electric energy density (2.9) then gives

$$w_{\text{elec}} = -\frac{\epsilon_0}{2r^2}\left(\frac{\mathrm{d}\Psi}{\mathrm{d}\alpha}\right)^2[\epsilon_\perp + \epsilon_a\sin^2\theta\sin^2\phi]. \tag{2.11}$$

The total energy density of the system will be given by $w = w_C + w_{\text{elec}}$ so that, by (2.7) and (2.11), the total energy $W = \int_V w\,\mathrm{d}V$ per unit depth in the z-direction is

$$\begin{aligned} W = \frac{1}{2}\ln\left(\frac{r_1}{r_0}\right)\int_0^\beta\Bigg[&-A_{11} + [(A_{12}+A_{11})\sin^4\phi + (A_{21}+A_{11})\cos^4\phi] \\ &+ \left(\frac{\mathrm{d}\phi}{\mathrm{d}\alpha}\right)^2[B_1\sin^2\phi + B_2\cos^2\phi] + 2\frac{\mathrm{d}\phi}{\mathrm{d}\alpha}[C_1\sin^2\phi - C_2\cos^2\phi]\cos\phi \\ &- \epsilon_0\left(\frac{\mathrm{d}\Psi}{\mathrm{d}\alpha}\right)^2[\epsilon_\perp + \epsilon_a\sin^2\theta\sin^2\phi]\Bigg]\mathrm{d}\alpha. \end{aligned} \tag{2.12}$$

The next step is to minimize the total energy in order to obtain the governing differential equations. In this case, since the above energy integral involves two different functions, namely ϕ and Ψ, two Euler–Lagrange equations must be solved simultaneously [26, p 198]:

$$\frac{\partial\bar{w}}{\partial\phi} - \frac{\mathrm{d}}{\mathrm{d}\alpha}\left(\frac{\partial\bar{w}}{\partial\phi'}\right) = 0, \qquad \frac{\partial\bar{w}}{\partial\Psi} - \frac{\mathrm{d}}{\mathrm{d}\alpha}\left(\frac{\partial\bar{w}}{\partial\Psi'}\right) = 0, \tag{2.13}$$

where $\bar{w}$ is the integrand appearing in (2.12) and a prime denotes differentiation with respect to α. Straightforward calculations then lead to the two governing equations

$$\begin{aligned} &2\sin\phi\cos\phi[(A_{12}+A_{11})\sin^2\phi - (A_{21}+A_{11})\cos^2\phi] - \left(\frac{\mathrm{d}\phi}{\mathrm{d}\alpha}\right)^2(B_1 - B_2)\sin\phi\cos\phi \\ &\quad - \frac{\mathrm{d}^2\phi}{\mathrm{d}\alpha^2}[B_1\sin^2\phi + B_2\cos^2\phi] - \left(\frac{\mathrm{d}\Psi}{\mathrm{d}\alpha}\right)^2\epsilon_0\epsilon_a\sin^2\theta\sin\phi\cos\phi = 0, \end{aligned} \tag{2.14}$$

and

$$\frac{\mathrm{d}}{\mathrm{d}\alpha}\left[\frac{\mathrm{d}\Psi}{\mathrm{d}\alpha}(\epsilon_\perp + \epsilon_a\sin^2\theta\sin^2\phi)\right] = 0. \tag{2.15}$$

Of course, in addition to solving these two differential equations, it is essential to ensure that Maxwell's equations ($\nabla\cdot\mathbf{D} = 0$, $\nabla\times\mathbf{E} = \mathbf{0}$, [25, p 495]) are satisfied. That which involves the curl of the electric field is easily verified and, by making use of equations (2.5), (2.8) and (2.10), it can be shown that the condition $\nabla\cdot\mathbf{D} = 0$ reduces to the same differential

equation given by (2.15). Thus we need only consider the coupled equations (2.14) and (2.15) as being sufficient for the problem to be discussed here.

In addition to the strong anchoring condition (2.4) for the angle ϕ, the applied voltage is taken to be zero volts on one bounding plate and V_{app} on the other. This leads to the boundary conditions

$$\Psi(0) = 0 \qquad \text{and} \qquad \Psi(\beta) = V_{\text{app}} \tag{2.16}$$

on the electric potential Ψ. Finally, in order to non-dimensionalize the governing equations, the scaled variables

$$\bar{\alpha} = \frac{\alpha}{\beta}, \qquad \bar{\Psi} = \frac{\Psi}{V_{\text{app}}} \tag{2.17}$$

are introduced allowing (2.14) and (2.15) to be written in the forms

$$\sin\phi\cos\phi[\mu_1\cos^2\phi + \mu_2\sin^2\phi] + \left(\frac{\mathrm{d}\phi}{\mathrm{d}\bar{\alpha}}\right)^2 \sigma\sin\phi\cos\phi + \frac{\mathrm{d}^2\phi}{\mathrm{d}\bar{\alpha}^2}[\sigma\sin^2\phi + 1] + \left(\frac{\mathrm{d}\bar{\Psi}}{\mathrm{d}\bar{\alpha}}\right)^2 U^2\sin\phi\cos\phi = 0, \tag{2.18}$$

and

$$\frac{\mathrm{d}}{\mathrm{d}\bar{\alpha}}\left[\frac{\mathrm{d}\bar{\Psi}}{\mathrm{d}\bar{\alpha}}(1 + \eta\sin^2\phi)\right] = 0, \tag{2.19}$$

where the dimensionless parameters are given by

$$\mu_1 = 2\beta^2\frac{(A_{21} + A_{11})}{B_2}, \qquad \mu_2 = -2\beta^2\frac{(A_{12} + A_{11})}{B_2}, \qquad \sigma = \frac{B_1}{B_2} - 1,$$
$$U^2 = \frac{\epsilon_0\epsilon_a V_{\text{app}}^2\sin^2\theta}{B_2}, \qquad \eta = \left(\frac{\epsilon_\parallel}{\epsilon_\perp} - 1\right)\sin^2\theta. \tag{2.20}$$

In addition to the main equations, the boundary conditions (2.4) and (2.16) must also be suitably scaled to give

$$\phi(0) = \phi(1) = 0, \qquad \bar{\Psi}(0) = 0, \qquad \bar{\Psi}(1) = 1. \tag{2.21}$$

Equations (2.18), (2.19) and (2.21) will form the basis for our investigation.

3. Small anisotropy approximation

It is known from earlier work by Carlsson *et al* [7] and Atkin and Stewart [9] that there is no distortion of the director until an applied voltage reaches a critical threshold. What is of interest here, however, is the behaviour of both the director orientation and the electric field once beyond this threshold. In this section, asymptotic series are employed to simplify the problem when the dielectric anisotropy is small. It will be shown that, when this is the case, the relevant solutions reduce to those obtained in [9] indicating that, for a small dielectric anisotropy η, the two-way coupling between liquid crystal and field can be neglected. We can suppose that the dielectric anisotropy η is small and insert expansions of the form

$$\phi(\bar{\alpha}) = \phi_0(\bar{\alpha}) + \eta\phi_1(\bar{\alpha}) + \eta^2\phi_2(\bar{\alpha}) + \eta^3\phi_3(\bar{\alpha}) + \cdots, \tag{3.1}$$

$$\bar{\Psi}(\bar{\alpha}) = \bar{\Psi}_0(\bar{\alpha}) + \eta\bar{\Psi}_1(\bar{\alpha}) + \eta^2\bar{\Psi}_2(\bar{\alpha}) + \eta^3\bar{\Psi}_3(\bar{\alpha}) + \cdots, \tag{3.2}$$

into the governing differential equations (2.18) and (2.19). Beyond the term of order η^0 the resulting terms become cumbersome and so only the first term in each of the expansions will

be sought. This procedure demonstrates that

$$\bar{\Psi}_0'' = 0, \tag{3.3}$$

and

$$\mu_1 \sin\phi_0 \cos^3\phi_0 + \mu_2 \sin^3\phi_0 \cos\phi_0 + \sigma \sin\phi_0 \cos\phi_0 (\phi_0')^2 + \sigma \sin^2\phi_0 \phi_0'' + \phi_0'' + U^2 \sin\phi_0 \cos\phi_0 (\bar{\Psi}_0')^2 = 0, \tag{3.4}$$

where a prime now denotes differentiation with respect to $\bar{\alpha}$. By the boundary conditions in (2.21), it is seen that the first term in the scaled potential is given by

$$\bar{\Psi}_0 = \bar{\alpha}, \tag{3.5}$$

which means, in terms of the original variables α and Ψ, that

$$\Psi_0 = \frac{\alpha}{\beta} V_{\text{app}}, \tag{3.6}$$

which leads to a uniform electric field, and, by (2.10), the electric field magnitude is given by [7]

$$E = -\frac{V_{\text{app}}}{r\beta}. \tag{3.7}$$

The differential equation (3.4) can be multiplied throughout by $2\phi_0'$ and then integrated to obtain

$$-\tfrac{1}{2}\mu_1 \cos^4\phi_0 + \tfrac{1}{2}\mu_2 \sin^4\phi_0 + (1 + \sigma \sin^2\phi_0)(\phi_0')^2 + U^2 \sin^2\phi_0 = C, \tag{3.8}$$

where C is a constant of integration. Now imposing the conditions [9]

$$\phi_0\left(\tfrac{1}{2}\right) = \phi_m, \qquad \phi_0'\left(\tfrac{1}{2}\right) = 0, \tag{3.9}$$

in order to obtain the constant C, it can be shown, via some rearrangement and integration, that $\phi_0(\bar{\alpha})$ is given implicitly by

$$\bar{\alpha} = \int_0^{\phi_0} \left[\frac{2(1 + \sigma \sin^2 u)}{\mu_1(\cos^4 u - \cos^4\phi_m) + \mu_2(\sin^4\phi_m - \sin^4 u) + 2U^2(\sin^2\phi_m - \sin^2 u)} \right]^{\frac{1}{2}} \mathrm{d}u. \tag{3.10}$$

Introducing the substitution

$$\sin u = \sin\phi_m \sin v, \tag{3.11}$$

and setting

$$\zeta(\bar{\alpha}) = \sin^{-1}\left(\frac{\sin\phi_0(\bar{\alpha})}{\sin\phi_m} \right), \tag{3.12}$$

then gives, after some cancellation,

$$\bar{\alpha} = \int_0^{\zeta} \left[\frac{2(1 + \sigma \sin^2\phi_m \sin^2 v)}{[2\mu_1 + 2U^2 + (\mu_2 - \mu_1)\sin^2\phi_m(1 + \sin^2 v)](1 - \sin^2\phi_m \sin^2 v)} \right]^{\frac{1}{2}} \mathrm{d}v, \tag{3.13}$$

which upon use of the conditions (3.9) results in an implicit equation for the maximum phase angle ϕ_m:

$$\frac{1}{2} = \int_0^{\frac{\pi}{2}} \left[\frac{2(1 + \sigma \sin^2\phi_m \sin^2 v)}{[2\mu_1 + 2U^2 + (\mu_2 - \mu_1)\sin^2\phi_m(1 + \sin^2 v)](1 - \sin^2\phi_m \sin^2 v)} \right]^{\frac{1}{2}} \mathrm{d}v. \tag{3.14}$$

We can suppose that $V_{\text{app}} \to V_c$ as we let $\phi_m \to 0$ on the right-hand side of (3.14) to recover the well-known critical Freedericksz threshold V_c for the onset of the Freedericksz transition

when the field is uniform, given by [9, 17]

$$\epsilon_a \epsilon_0 V_c^2 \sin^2\theta = \pi^2 B_2 - 2\beta^2(A_{21} + A_{11}), \tag{3.15}$$

and record that this implies that the critical electric field magnitude is given by

$$E_c = -\frac{1}{r\beta} V_c. \tag{3.16}$$

Returning to equation (3.10), it can finally be shown that, by converting back to the original variable α and reintroducing the material parameters (2.20), we obtain the same solution as that found by Atkin and Stewart [9, equation (36)]. This should be expected for the first term of the expansion in ϕ, since the first term in the potential series gave rise to a uniform field which was the situation considered in [9]. The advantage of looking at the problem in terms of an asymptotic series, however, is that it gives justification for neglecting the nonlinear coupling between liquid crystal and field when the dielectric anisotropy is small.

4. Low field regime

Our next investigation looks at when the applied voltage is just above this critical threshold. In this case we introduce a small perturbation δ through the relation [19]

$$U = \rho(1 - \rho\delta^2)^{-1}, \qquad \text{where} \qquad \rho^2 = B_2^{-1}[\pi^2 B_2 - 2\beta^2(A_{21} + A_{11})]. \tag{4.1}$$

This particular way of expressing the increase in V_{app} above V_c (defined by in (3.15)) allows the series expansions that appear in the calculations below to be more tractable in terms of δ. It is seen that $\delta = 0$ corresponds to $U = \rho$, which, by (2.20) in turn corresponds to $V_{\text{app}} = V_c$; a small increase in δ corresponds to a small increase in the voltage above V_c.

It is reasonable to assume that ϕ and δ are small enough so that the following approximations are valid:

$$\begin{aligned} &\sin^2\phi \approx \phi^2 - \tfrac{1}{3}\phi^4, && \cos^2\phi \approx 1 - \phi^2 + \tfrac{1}{3}\phi^4, \\ &\sin\phi\cos\phi \approx \phi - \tfrac{2}{3}\phi^3, && (1 - \rho\delta^2)^{-2} \approx 1 + 2\rho\delta^2 + 3\rho^2\delta^4. \end{aligned} \tag{4.2}$$

Before introducing general series expressions it is worth realizing that as $\delta \to 0$ then it must be the case that $\phi \to 0$ also. This means that any series for the director rotation cannot have a term that is independent of δ. Therefore we employ series solutions for the phase angle and normalized potential of the form

$$\phi(\bar{\alpha}) = \delta\phi_1(\bar{\alpha}) + \delta^2\phi_2(\bar{\alpha}) + \delta^3\phi_3(\bar{\alpha}) + \delta^4\phi_4(\bar{\alpha}) + \cdots \tag{4.3}$$

$$\bar{\Psi}(\bar{\alpha}) = \bar{\Psi}_0(\bar{\alpha}) + \delta\bar{\Psi}_1(\bar{\alpha}) + \delta^2\bar{\Psi}_2(\bar{\alpha}) + \delta^3\bar{\Psi}_3(\bar{\alpha}) + \delta^4\bar{\Psi}_4(\bar{\alpha}) + \cdots. \tag{4.4}$$

By inserting the above series expansions into the governing equations (2.18) and (2.19) and making use of the approximations in (4.2) it is possible to show that, up to fourth order in δ, we have

$$\begin{aligned} &\delta\big[\mu_1\phi_1 + \phi_1'' + \rho^2\phi_1\bar{\Psi}_0'^2\big] + \delta^2\big[\mu_1\phi_2 + \phi_2'' + 2\rho^2\phi_1\bar{\Psi}_0'\bar{\Psi}_1' + \rho^2\phi_2\bar{\Psi}_0'^2\big] \\ &\quad + \delta^3\big[\mu_1\phi_3 + \big(\mu_2 - \tfrac{5}{3}\mu_1\big)\phi_1^3 + \sigma\phi_1\phi_1'^2 + \sigma\phi_1^2\phi_1'' + \phi_3'' + \rho^2\phi_1\bar{\Psi}_1'^2 \\ &\quad + 2\rho^2\phi_1\bar{\Psi}_0'\bar{\Psi}_2' + 2\rho^2\phi_2\bar{\Psi}_0'\bar{\Psi}_1' + \rho^2\phi_3\bar{\Psi}_0'^2 - \tfrac{2}{3}\rho^2\phi_1^3\bar{\Psi}_0'^2 + 2\rho^3\phi_1\bar{\Psi}_0'^2\big] \\ &\quad + \delta^4\big[\mu_1\phi_4 + (3\mu_2 - 5\mu_1)\phi_1^2\phi_2 + 2\sigma\phi_1\phi_1'\phi_2' + \sigma\phi_2\phi_1'^2 + \sigma\phi_1^2\phi_2'' \\ &\quad + 2\sigma\phi_1\phi_2\phi_1'' + \phi_4'' + 2\rho^2\phi_1\bar{\Psi}_1'\bar{\Psi}_2' + 2\rho^2\phi_1\bar{\Psi}_0'\bar{\Psi}_3' + \rho^2\phi_2\bar{\Psi}_1'^2 + 2\rho^2\phi_2\bar{\Psi}_0'\bar{\Psi}_2' \\ &\quad + 2\rho^2\phi_3\bar{\Psi}_0'\bar{\Psi}_1' + \rho^2\phi_4\bar{\Psi}_0'^2 - \tfrac{4}{3}\rho^2\phi_1^3\bar{\Psi}_0'\bar{\Psi}_1' - 2\rho^2\phi_1^2\phi_2\bar{\Psi}_0'^2 + 4\rho^3\phi_1\bar{\Psi}_0'\bar{\Psi}_1' \\ &\quad + 2\rho^3\phi_2\bar{\Psi}_0'^2\big] = 0, \end{aligned} \tag{4.5}$$

and

$$\bar{\Psi}_0'' + \delta\bar{\Psi}_1'' + \delta^2\left[\eta\phi_1^2\bar{\Psi}_0' + \bar{\Psi}_2'\right]' + \delta^3\left[2\eta\phi_1\phi_2\bar{\Psi}_0' + \eta\phi_1^2\bar{\Psi}_1' + \bar{\Psi}_3'\right]' + \delta^4\left[2\eta\phi_1\phi_3\bar{\Psi}_0' + \eta\phi_2^2\bar{\Psi}_0' - \tfrac{1}{3}\eta\phi_1^4\bar{\Psi}_0' + 2\eta\phi_1\phi_2\bar{\Psi}_1' + \eta\phi_1^2\bar{\Psi}_2' + \bar{\Psi}_4'\right]' = 0. \quad (4.6)$$

Similarly, the boundary conditions (2.21) become

$$\begin{aligned} &\phi_1(0) = \phi_2(0) = \phi_3(0) = \phi_4(0) = 0,\\ &\phi_1(1) = \phi_2(1) = \phi_3(1) = \phi_4(1) = 0,\\ &\bar{\Psi}_0(0) = \bar{\Psi}_1(0) = \bar{\Psi}_2(0) = \bar{\Psi}_3(0) = \bar{\Psi}_4(0) = 0, \quad (4.7)\\ &\bar{\Psi}_0(1) = 1,\\ &\bar{\Psi}_1(1) = \bar{\Psi}_2(1) = \bar{\Psi}_3(1) = \bar{\Psi}_4(1) = 0. \end{aligned}$$

We can now systematically solve equations (4.5) and (4.6) (by setting the coefficients of each order of δ to zero, to obtain simpler differential equations) subject to the boundary conditions (4.7) in order to obtain the functions ϕ_i and $\bar{\Psi}_i$. Starting with the coefficient of δ^0 in equation (4.6) and then subsequently using the coefficients of δ in (4.5) and (4.6), and δ^2 in (4.5) and (4.6), leads to the results:

$$\bar{\Psi}_0 = \bar{\alpha}, \qquad \bar{\Psi}_1 = 0, \qquad \bar{\Psi}_2 = \frac{c_1^2\eta}{2\pi}\sin(\pi\bar{\alpha})\cos(\pi\bar{\alpha}), \quad (4.8)$$

$$\phi_1 = c_1\sin(\pi\bar{\alpha}), \qquad \phi_2 = c_2\sin(\pi\bar{\alpha}), \quad (4.9)$$

where the constants c_1 and c_2 are to be determined. It is worth noting from equations (2.20) and (4.1) that $\mu_1 + \rho^2 = \pi^2$ when deriving these equations.

The procedure to obtain ϕ_3 and $\bar{\Psi}_3$ remains the same as above; however, more detailed manipulation of the associated differential equations is needed. The coefficient of δ^3 in (4.5) when set to zero gives rise to the differential equation

$$\phi_3'' + \pi^2\phi_3 + \xi_1 c_1^3\sin^3(\pi\bar{\alpha}) + \left(\xi_2 c_1^3 + \xi_3 c_1\right)\sin(\pi\bar{\alpha}) = 0, \quad (4.10)$$

where we have set

$$\xi_1 = \mu_2 - \mu_1 - \tfrac{2}{3}\pi^2 - 2\sigma\pi^2 - 2\rho^2\eta, \qquad \xi_2 = \sigma\pi^2 + \rho^2\eta, \qquad \xi_3 = 2\rho^3. \quad (4.11)$$

Solving (4.10) subject to the conditions in (4.7) then gives the result (assuming that $c_1 \neq 0$)

$$c_1^2 = \frac{8\rho^3}{3(\mu_1 - \mu_2) + 2\pi^2(1+\sigma) + 2\rho^2\eta} \equiv \lambda, \quad (4.12)$$

which leads to the solutions

$$\phi_3 = c_3\sin(\pi\bar{\alpha}) \pm \frac{\xi_1\lambda^{\frac{3}{2}}}{32\pi^2}\sin(3\pi\bar{\alpha}), \quad (4.13)$$

with c_3 representing another integration constant. From the coefficient of δ^3 in (4.6) it is straightforward to find that

$$\bar{\Psi}_3 = \pm\frac{c_2\eta\lambda^{\frac{1}{2}}}{\pi}\sin(\pi\bar{\alpha})\cos(\pi\bar{\alpha}). \quad (4.14)$$

Finally, the coefficient of δ^4 in (4.5) set equal to zero gives an equation for ϕ_4, namely,

$$\phi_4'' + \pi^2\phi_4 + \xi_4 c_2\sin^3(\pi\bar{\alpha}) + \xi_5 c_2\sin(\pi\bar{\alpha}) = 0, \quad (4.15)$$

where

$$\xi_4 = (3\mu_2 - 3\mu_1 - 2\pi^2 - 6\sigma\pi^2 - 6\rho^2\eta)\lambda, \qquad \xi_5 = 3\sigma\pi^2\lambda + 2\rho^3 + 3\rho^2\eta\lambda. \quad (4.16)$$

Solving this equation leads to the conclusion that $c_2 = 0$ and that ϕ_4 must be given by

$$\phi_4 = c_4 \sin(\pi\bar{\alpha}), \tag{4.17}$$

with c_4 being a constant of integration.

This now allows us to write down the asymptotic expansions up to at least order δ^2 for $\phi(\bar{\alpha})$ and $\bar{\Psi}(\bar{\alpha})$. Without loss of generality, we shall select the plus sign in (4.12) to find that

$$\phi(\bar{\alpha}) = \delta\sqrt{\lambda}\sin(\pi\bar{\alpha}) + O(\delta^3), \tag{4.18}$$

$$\bar{\Psi}(\bar{\alpha}) = \bar{\alpha} + \delta^2\frac{\eta\lambda}{2\pi}\sin(\pi\bar{\alpha})\cos(\pi\bar{\alpha}) + O(\delta^4). \tag{4.19}$$

(The solutions with the minus signs correspond to a rotation of the director in the opposite direction.) Finally, we transform the above two equations using (2.17) in order to obtain

$$\phi(\alpha) = \delta\sqrt{\lambda}\sin\left(\frac{\pi\alpha}{\beta}\right) + O(\delta^3), \tag{4.20}$$

and

$$\Psi(\alpha) = \left[\frac{\alpha}{\beta} + \delta^2\frac{\eta\lambda}{2\pi}\sin\left(\frac{\pi\alpha}{\beta}\right)\cos\left(\frac{\pi\alpha}{\beta}\right) + O(\delta^4)\right]V_{\text{app}}. \tag{4.21}$$

Although equation (4.21) determines the electric potential throughout the wedge cell, it is of more use to revert to an expression for the electric field so that a comparison of results can be made with the full solution found in Smith and Stewart [17]. Using equation (2.10) it is straightforward to show that the electric field is given by

$$\mathbf{E} = -\widehat{\boldsymbol{\alpha}}\frac{V_{\text{app}}}{r\beta}\left[1 + \delta^2\frac{\eta\lambda}{2}\cos\left(\frac{2\pi\alpha}{\beta}\right) + O(\delta^4)\right]. \tag{4.22}$$

Normalizing with respect to the critical field in (3.16) allows the r-dependence to be eliminated, giving

$$\frac{E}{E_c} = \frac{V_{\text{app}}}{V_c}\left[1 + \delta^2\frac{\eta\lambda}{2}\cos\left(\frac{2\pi\alpha}{\beta}\right) + O(\delta^4)\right], \tag{4.23}$$

where $E = |\mathbf{E}|$. In order to plot solutions it is particularly useful to be able to select a value for the voltage ratio V_{app}/V_c rather than a value for δ, and so by making use of the critical voltage (3.15), the non-dimensional parameter U in $(2.20)_4$ and the expression $(4.1)_1$, it is convenient to note that

$$\delta^2 = \frac{1}{\rho}\left(1 - \frac{V_c}{V_{\text{app}}}\right), \tag{4.24}$$

where ρ is defined in equation $(4.1)_2$. Figures 3–5 show how the director and field vary across the wedge for a variety of voltage ratios, permittivity values and elastic constants. In each of these figures the dashed curves are the asymptotic solutions ((4.20) or (4.23)) and, for comparison, the numerical solutions obtained using the method outlined by Smith and Stewart [17] are given as solid curves. For realistic parameter values we combined the experimental results for $A_{11} + A_{21}$ obtained from a wedge experiment by Findon and Gleeson [22] with other data available from [27–29]. Unless otherwise noted in the figure captions, the data used are

$$\begin{aligned}
&\beta = 2\times10^{-3}\ \text{rad}, && B_1 = 7.02\times10^{-12}\ \text{N}, && B_2 = 3.51\times10^{-12}\ \text{N},\\
&\epsilon_\perp = 2.91, && \epsilon_\parallel = 3.89, && \theta = \frac{2\pi}{15}\ \text{rad},\\
&A_{11} = -1.44\times10^{-4}\ \text{N}, && A_{12} = 1.711\times10^{-4}\ \text{N}, && A_{21} = 1.212\times10^{-4}\ \text{N}.
\end{aligned} \tag{4.25}$$

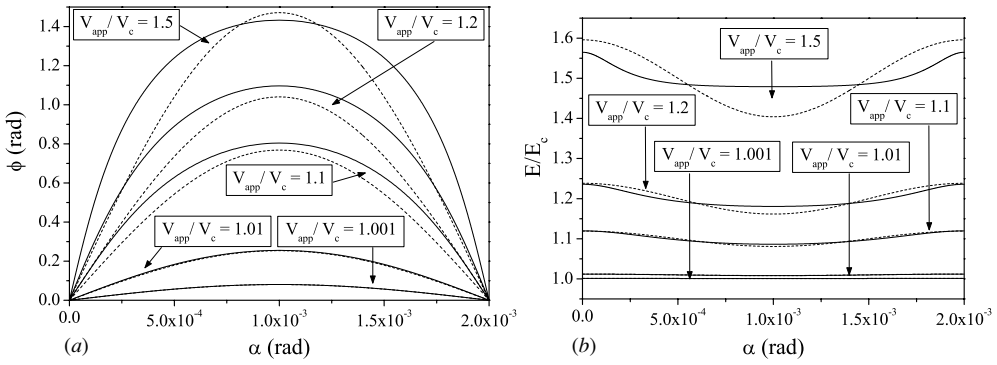

Figure 3. (*a*) Director behaviour and (*b*) field distortion across the SmC wedge for different applied voltage ratios, with the dashed and solid curves representing the asymptotic and numerical solutions, respectively. The parameter values are given by (4.25).

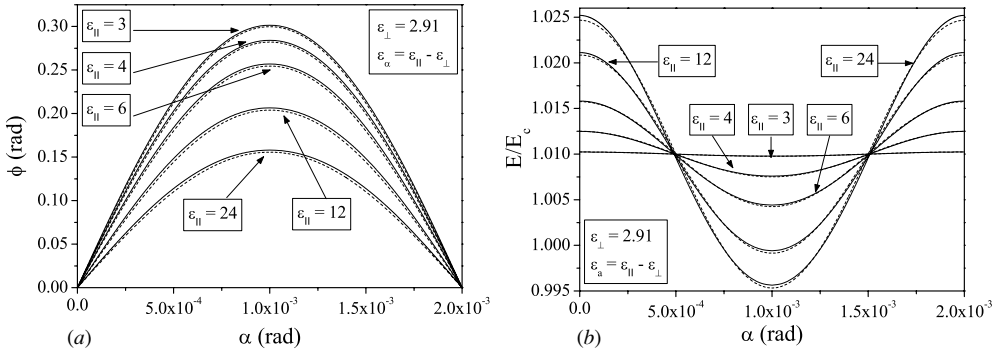

Figure 4. (*a*) Director behaviour and (*b*) field distortion across the SmC wedge for different values of $\epsilon_\parallel$ when $V_{\rm app}/V_c = 1.01$, with the dashed and solid curves representing the asymptotic and numerical solutions, respectively. The parameter values are given by (4.25) except that here $B_1 = B_2 = 5 \times 10^{-12}$ N.

From figure 3 it is clear to see, for the data used, that the asymptotic expansions provide accurate approximations to the solutions when the voltage is just slightly above threshold. It is only when the voltage ratio becomes greater than about 1.1 that the asymptotic solutions significantly diverge from the full numerical solutions. As can be seen from figures 4 and 5, varying any of the material parameters, $\epsilon_\parallel$, B_1 or B_2, does not appear to have much effect on the accuracy of the asymptotic solutions, as is expected.

5. High field regime

In the previous section, asymptotic solutions were obtained which described the director and field behaviour when a voltage just larger than that at threshold was applied to the SmC wedge. In this section our attention shifts to the case of a high voltage being applied to the cell. Although assumptions are made regarding the magnitudes of some of the non-dimensionalized material parameters, they are not seen as being too restrictive when applying realistic data to the final asymptotic solutions. Due to the nature of the problem it is convenient to construct

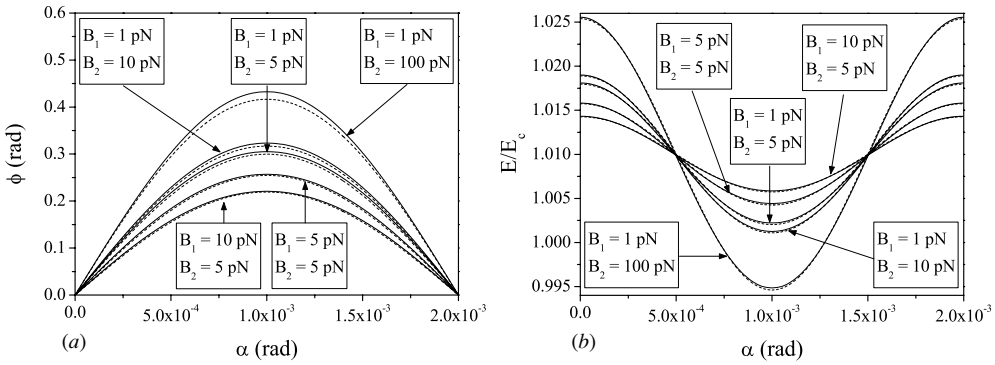

Figure 5. (*a*) Director behaviour and (*b*) field distortion across the SmC wedge for different values of B_1 and B_2, with the dashed and solid curves representing the asymptotic and numerical solutions, respectively. In this case $\epsilon_{\|} = 6$ and $V_{\text{app}}/V_c = 1.01$ with the remaining parameters given by (4.25).

two separate types of approximate solutions in sections 5.1 and 5.2 that will be matched together in section 5.3. In section 5.1 outer solutions are obtained which demonstrate the behaviour of the director and field at points far from the boundaries while inner solutions are determined in section 5.2 which dictate the behaviour near the boundaries.

5.1. The outer solutions

In this case we set

$$U = \frac{1}{\epsilon}, \qquad \sigma = \epsilon\bar{\sigma}, \qquad \eta = \epsilon\bar{\eta}, \qquad \bar{\sigma}, \bar{\eta} = O(1), \tag{5.1}$$

where ϵ is some small positive parameter ($\epsilon \ll 1$). Inserting the expansions

$$\phi(\bar{\alpha}) = \phi_0(\bar{\alpha}) + \epsilon\phi_1(\bar{\alpha}) + \epsilon^2\phi_2(\bar{\alpha}) + \epsilon^3\phi_3(\bar{\alpha}) + \cdots, \tag{5.2}$$

$$\bar{\Psi}(\bar{\alpha}) = \bar{\Psi}_0(\bar{\alpha}) + \epsilon\bar{\Psi}_1(\bar{\alpha}) + \epsilon^2\bar{\Psi}_2(\bar{\alpha}) + \epsilon^3\bar{\Psi}_3(\bar{\alpha}) + \cdots, \tag{5.3}$$

into the main governing equations (2.18) and (2.19) and then expanding up to order ϵ^2 shows that we require

$$\begin{aligned}\sin\phi_0\cos\phi_0\bar{\Psi}_{0\bar{\alpha}}^2 + \epsilon\big[&2\sin\phi_0\cos\phi_0\bar{\Psi}_{0\bar{\alpha}}\bar{\Psi}_{1\bar{\alpha}} - \phi_1\sin^2\phi_0\bar{\Psi}_{0\bar{\alpha}}^2 + \phi_1\cos^2\phi_0\bar{\Psi}_{0\bar{\alpha}}^2\big]\\ &+\epsilon^2\big[\sin\phi_0\cos\phi_0\left(\mu_1\cos^2\phi_0 + \mu_2\sin^2\phi_0\right) + \phi_{0\bar{\alpha}\bar{\alpha}} + \sin\phi_0\cos\phi_0\bar{\Psi}_{1\bar{\alpha}}^2\\ &+2\sin\phi_0\cos\phi_0\bar{\Psi}_{0\bar{\alpha}}\bar{\Psi}_{2\bar{\alpha}} - 2\phi_1^2\sin\phi_0\cos\phi_0\bar{\Psi}_{0\bar{\alpha}}^2 - 2\phi_1\sin^2\phi_0\bar{\Psi}_{0\bar{\alpha}}\bar{\Psi}_{1\bar{\alpha}}\\ &-\phi_2\sin^2\phi_0\bar{\Psi}_{0\bar{\alpha}}^2 + 2\phi_1\cos^2\phi_0\bar{\Psi}_{0\bar{\alpha}}\bar{\Psi}_{1\bar{\alpha}} + \phi_2\cos^2\phi_0\bar{\Psi}_{0\bar{\alpha}}^2\big] = 0,\end{aligned} \tag{5.4}$$

and

$$\bar{\Psi}_{0\bar{\alpha}\bar{\alpha}} + \epsilon[\bar{\eta}\sin^2\phi_0\bar{\Psi}_{0\bar{\alpha}} + \bar{\Psi}_{1\bar{\alpha}}]_{\bar{\alpha}} + \epsilon^2[2\bar{\eta}\phi_1\sin\phi_0\cos\phi_0\bar{\Psi}_{0\bar{\alpha}} + \bar{\eta}\sin^2\phi_0\bar{\Psi}_{1\bar{\alpha}} + \bar{\Psi}_{2\bar{\alpha}}]_{\bar{\alpha}} = 0, \tag{5.5}$$

where the trigonometric functions have been expanded via the approximations

$$\sin\phi \approx \left(1 - \tfrac{1}{2}\epsilon^2\phi_1^2\right)\sin\phi_0 + (\epsilon\phi_1 + \epsilon^2\phi_2)\cos\phi_0, \tag{5.6}$$

$$\cos\phi \approx \left(1 - \tfrac{1}{2}\epsilon^2\phi_1^2\right)\cos\phi_0 - (\epsilon\phi_1 + \epsilon^2\phi_2)\sin\phi_0. \tag{5.7}$$

It should be noted that in these equations the subscripts that involve $\bar{\alpha}$ indicate differentiation. This notation has been introduced instead of the primes from section 4 in order to avoid confusion with the different derivatives that will appear when considering the inner solutions below.

In order to obtain the outer solution, each coefficient of the powers of ϵ in (5.4) and (5.5) must be set equal to zero and solved sequentially for the various ϕ_i and $\bar{\Psi}_i$. Since this situation deals with the outer solution it is not possible to use the boundary conditions. To achieve a full solution then requires the introduction of some other condition. Due to the symmetry of the wedge around $\alpha = \frac{\beta}{2}\left(\bar{\alpha} = \frac{1}{2}\right)$ and the reasonable expectation that the potential is a monotonically increasing function of distance, it is natural to suppose that the potential must reach half of the applied voltage along the line $\alpha = \frac{\beta}{2}$. This condition can therefore be stated as

$$\bar{\Psi}_0\left(\tfrac{1}{2}\right) = \tfrac{1}{2}, \qquad \bar{\Psi}_1\left(\tfrac{1}{2}\right) = \bar{\Psi}_2\left(\tfrac{1}{2}\right) = 0. \tag{5.8}$$

First, the coefficient of ϵ^0 in equation (5.5) set to zero under the conditions stated in (5.8) then gives

$$\bar{\Psi}_0 = (1 - 2b_0)\,\bar{\alpha} + b_0, \tag{5.9}$$

where b_0 is a constant of integration yet to be determined. Next, looking at the coefficient of ϵ^0 in (5.4) shows that ϕ_0 must be a half integer multiple of π; however, we choose the physically most relevant one, namely $\phi_0 = \frac{\pi}{2}$. Similarly, from the coefficients of ϵ and ϵ^2 in equations (5.4) and (5.5), and applying the conditions in (5.8), it can be shown that

$$\bar{\Psi}_1 = -2b_1\bar{\alpha} + b_1, \qquad \bar{\Psi}_2 = -2b_2\bar{\alpha} + b_2, \tag{5.10}$$

$$\phi_1 = 0, \qquad \phi_2 = 0, \tag{5.11}$$

where b_1 and b_2 are constants of integration. Combining all of these results gives the full outer solutions up to at least second order in ϵ as

$$\phi = \frac{\pi}{2}, \tag{5.12}$$

and

$$\bar{\Psi} = (1 - 2b_0)\,\bar{\alpha} + b_0 + \epsilon\,(-2b_1\bar{\alpha} + b_1) + \epsilon^2\,(-2b_2\bar{\alpha} + b_2)\,. \tag{5.13}$$

5.2. The inner solutions

To consider the inner 'boundary layer' solution it is first essential to rescale $\bar{\alpha}$ so that

$$\bar{\alpha} = \epsilon\hat{\alpha}, \qquad \hat{\alpha} = O(1), \tag{5.14}$$

where ϵ is the small parameter introduced previously. Changing to this new variable, in addition to substituting the parameters (5.1) into the governing equations (2.18) and (2.19), then leads, after introducing expansions of the form (5.2) and (5.3) (with $\bar{\alpha}$ replaced with $\hat{\alpha}$) and straightforward manipulation, to the differential equations set out below in (5.15) and (5.16). In order to obtain sufficient information for a reasonably accurate solution, equation (2.18) is expanded up to third order in ϵ whereas equation (2.19) needs to be expanded only to second order.

$$\begin{aligned}\sin\phi_0\cos\phi_0\bar{\Psi}_{0\hat{\alpha}}^2 + \epsilon\big[&2\sin\phi_0\cos\phi_0\bar{\Psi}_{0\hat{\alpha}}\bar{\Psi}_{1\hat{\alpha}} - \phi_1\sin^2\phi_0\bar{\Psi}_{0\hat{\alpha}}^2 + \phi_1\cos^2\phi_0\bar{\Psi}_{0\hat{\alpha}}^2\big] \\ &+ \epsilon^2\big[\phi_{0\hat{\alpha}\hat{\alpha}} + 2\sin\phi_0\cos\phi_0\bar{\Psi}_{0\hat{\alpha}}\bar{\Psi}_{2\hat{\alpha}} + \sin\phi_0\cos\phi_0\bar{\Psi}_{1\hat{\alpha}}^2 - 2\phi_1^2\sin\phi_0\cos\phi_0\bar{\Psi}_{0\hat{\alpha}}^2\end{aligned}$$

$$
\begin{aligned}
&- 2\phi_1 \sin^2\phi_0 \bar{\Psi}_{0\hat{\alpha}} \bar{\Psi}_{1\hat{\alpha}} - \phi_2 \sin^2\phi_0 \bar{\Psi}^2_{0\hat{\alpha}} + 2\phi_1 \cos^2\phi_0 \bar{\Psi}_{0\hat{\alpha}} \bar{\Psi}_{1\hat{\alpha}} + \phi_2 \cos^2\phi_0 \bar{\Psi}^2_{0\hat{\alpha}}\big] \\
&+ \epsilon^3\big[\bar{\sigma} \sin\phi_0 \cos\phi_0 \phi^2_{0\hat{\alpha}} + \bar{\sigma} \sin^2\phi_0 \phi_{0\hat{\alpha}\hat{\alpha}} + \phi_{1\hat{\alpha}\hat{\alpha}} + 2\sin\phi_0 \cos\phi_0 \bar{\Psi}_{0\hat{\alpha}} \bar{\Psi}_{3\hat{\alpha}} \\
&+ 2\sin\phi_0 \cos\phi_0 \bar{\Psi}_{1\hat{\alpha}} \bar{\Psi}_{2\hat{\alpha}} - 4\phi_1^2 \sin\phi_0 \cos\phi_0 \bar{\Psi}_{0\hat{\alpha}} \bar{\Psi}_{1\hat{\alpha}} - 4\phi_1\phi_2 \sin\phi_0 \cos\phi_0 \bar{\Psi}^2_{0\hat{\alpha}} \\
&- 2\phi_1 \sin^2\phi_0 \bar{\Psi}_{0\hat{\alpha}} \bar{\Psi}_{2\hat{\alpha}} - \phi_1 \sin^2\phi_0 \bar{\Psi}^2_{1\hat{\alpha}} - 2\phi_2 \sin^2\phi_0 \bar{\Psi}_{0\hat{\alpha}} \bar{\Psi}_{1\hat{\alpha}} - \phi_3 \sin^2\phi_0 \bar{\Psi}^2_{0\hat{\alpha}} \\
&+ \tfrac{2}{3}\phi_1^3 \sin^2\phi_0 \bar{\Psi}^2_{0\hat{\alpha}} + 2\phi_1 \cos^2\phi_0 \bar{\Psi}_{0\hat{\alpha}} \bar{\Psi}_{2\hat{\alpha}} + \phi_1 \cos^2\phi_0 \bar{\Psi}^2_{1\hat{\alpha}} - \tfrac{2}{3}\phi_1^3 \cos^2\phi_0 \bar{\Psi}^2_{0\hat{\alpha}} \\
&+ 2\phi_2 \cos^2\phi_0 \bar{\Psi}_{0\hat{\alpha}} \bar{\Psi}_{1\hat{\alpha}} + \phi_3 \cos^2\phi_0 \bar{\Psi}^2_{0\hat{\alpha}}\big] = 0, \qquad (5.15)
\end{aligned}
$$

$$
\bar{\Psi}_{0\hat{\alpha}\hat{\alpha}} + \epsilon[\bar{\eta} \sin^2\phi_0 \bar{\Psi}_{0\hat{\alpha}} + \bar{\Psi}_{1\hat{\alpha}}]_{\hat{\alpha}} + \epsilon^2[2\bar{\eta}\phi_1 \sin\phi_0 \cos\phi_0 \bar{\Psi}_{0\hat{\alpha}} + \bar{\eta} \sin^2\phi_0 \bar{\Psi}_{1\hat{\alpha}} + \bar{\Psi}_{2\hat{\alpha}}]_{\hat{\alpha}} = 0. \qquad (5.16)
$$

In the above two equations the following approximations were imposed on the trigonometric functions:

$$
\sin\phi \approx \left(1 - \tfrac{1}{2}\epsilon^2\phi_1^2 - \epsilon^3\phi_1\phi_2\right)\sin\phi_0 + \left(\epsilon\phi_1 + \epsilon^2\phi_2 + \epsilon^3\phi_3 - \tfrac{1}{6}\epsilon^3\phi_1^3\right)\cos\phi_0, \qquad (5.17)
$$

$$
\cos\phi \approx \left(1 - \tfrac{1}{2}\epsilon^2\phi_1^2 - \epsilon^3\phi_1\phi_2\right)\cos\phi_0 - \left(\epsilon\phi_1 + \epsilon^2\phi_2 + \epsilon^3\phi_3 - \tfrac{1}{6}\epsilon^3\phi_1^3\right)\sin\phi_0. \qquad (5.18)
$$

Although boundary layers exist at both plates that form the wedge, due to symmetry properties it is only necessary to obtain a solution for one of these regions. From the scaling chosen in equation (5.14) it is clear that the calculations above will lead to the solution on the lower boundary where

$$
\phi_0(0) = \phi_1(0) = \phi_2(0) = \phi_3(0) = 0, \qquad \bar{\Psi}_0(0) = \bar{\Psi}_1(0) = \bar{\Psi}_2(0) = 0. \qquad (5.19)
$$

Also, as $\hat{\alpha} \to \infty$ the inner solution must tend towards the outer solution and so

$$
\begin{aligned}
&\lim_{\hat{\alpha}\to\infty} \phi_0 = \frac{\pi}{2}, \qquad \lim_{\hat{\alpha}\to\infty} \phi_1 = \lim_{\hat{\alpha}\to\infty} \phi_2 = \lim_{\hat{\alpha}\to\infty} \phi_3 = 0, \\
&\lim_{\hat{\alpha}\to\infty} \phi_{0\hat{\alpha}} = \lim_{\hat{\alpha}\to\infty} \phi_{1\hat{\alpha}} = \lim_{\hat{\alpha}\to\infty} \phi_{2\hat{\alpha}} = \lim_{\hat{\alpha}\to\infty} \phi_{3\hat{\alpha}} = 0.
\end{aligned} \qquad (5.20)
$$

Once again, setting coefficients of each power of ϵ in equations (5.15) and (5.16) to zero allows us to obtain, via the above boundary conditions (5.19) and (5.20), solutions for the functions $\phi_i(\hat{\alpha})$ and $\bar{\Psi}_i(\hat{\alpha})$. Starting with the coefficient of ϵ^0 in (5.16) immediately gives

$$
\bar{\Psi}_0 = a_0\hat{\alpha}, \qquad (5.21)
$$

however the coefficient of ϵ^0 in (5.15) forces a_0 to be zero, via the boundary conditions (5.19) and (5.20) and therefore,

$$
\bar{\Psi}_0 = 0. \qquad (5.22)
$$

From the ϵ term in (5.16) it is clear that

$$
\bar{\Psi}_1 = a_1\hat{\alpha}, \qquad (5.23)
$$

where a_1 is an integration constant to be determined. The term involving ϵ in (5.15) gives no information and so attention shifts to the coefficient of ϵ^2 which results in the differential equation

$$
\phi^2_{0\hat{\alpha}} = a_1^2 \cos^2\phi_0 + \bar{a}_0, \qquad (5.24)
$$

where $\bar{a}_0$ is a constant of integration. Using condition (5.20) on equation (5.24), along with standard integration techniques, results in the solution

$$
\phi_0 = 2\tan^{-1}(\exp(a_1\hat{\alpha})) - \frac{\pi}{2}. \qquad (5.25)
$$

By using standard trigonometric identities and basic geometrical considerations, the cosine and sine of ϕ_0 can be written as

$$\sin\phi_0 = \tanh(a_1\hat{\alpha}), \qquad \cos\phi_0 = \operatorname{sech}(a_1\hat{\alpha}). \tag{5.26}$$

Making use of this in the coefficient of ϵ^2 in equation (5.16) allows straightforward integration to give

$$\bar{\Psi}_2 = a_2\hat{\alpha} - \bar{\eta}a_1\hat{\alpha} + \bar{\eta}\tanh(a_1\hat{\alpha}), \tag{5.27}$$

where a_2 is another integration constant. Returning to (5.15), the differential equation arising from the coefficient of ϵ^3 can be rearranged, making use of (5.24) and $(5.26)_2$, in order to obtain

$$\begin{aligned}\phi_{1\hat{\alpha}\hat{\alpha}} + a_1^2\cos(2\phi_0)\phi_1 = {} & -\bar{\sigma}\sin\phi_0\cos\phi_0\phi_{0\hat{\alpha}}^2 - \bar{\sigma}\sin^2\phi_0\phi_{0\hat{\alpha}\hat{\alpha}} \\ & - 2a_1(a_2 - \bar{\eta}a_1)\sin\phi_0\cos\phi_0 + 2\bar{\eta}\cos^2\phi_0\phi_{0\hat{\alpha}\hat{\alpha}}.\end{aligned} \tag{5.28}$$

To solve this differential equation it is imperative to put it into a more convenient and standard form. To do this we can rewrite the trigonometric functions in terms of exponentials and then convert to a differential equation involving hyperbolic functions. Elementary calculations applied to equation (5.25) show that

$$\begin{aligned}&\sin\phi_0 = \frac{\exp(a_1\hat{\alpha}) - \exp(-a_1\hat{\alpha})}{\exp(a_1\hat{\alpha}) + \exp(-a_1\hat{\alpha})}, \qquad \cos\phi_0 = \frac{2}{\exp(a_1\hat{\alpha}) + \exp(-a_1\hat{\alpha})}, \\ &\cos(2\phi_0) = \frac{8\exp(2a_1\hat{\alpha})}{(1+\exp(2a_1\hat{\alpha}))^2} - 1, \qquad \phi_{0\hat{\alpha}} = \frac{2a_1\exp(a_1\hat{\alpha})}{1+\exp(2a_1\hat{\alpha})}, \\ &\phi_{0\hat{\alpha}\hat{\alpha}} = \frac{2a_1^2(\exp(a_1\hat{\alpha}) - \exp(3a_1\hat{\alpha}))}{(1+\exp(2a_1\hat{\alpha}))^2}.\end{aligned} \tag{5.29}$$

Inserting these into (5.28) finally leads to

$$\phi_{1\hat{\alpha}\hat{\alpha}} + a_1^2(2\operatorname{sech}^2(a_1\hat{\alpha}) - 1)\phi_1 = \frac{\lambda_1\sinh(3a_1\hat{\alpha}) + \lambda_2\sinh(a_1\hat{\alpha})}{4\cosh^4(a_1\hat{\alpha})}, \tag{5.30}$$

where

$$\lambda_1 = -a_1(2a_2 - 2\bar{\eta}a_1 - \bar{\sigma}a_1), \qquad \lambda_2 = -a_1(7\bar{\sigma}a_1 + 6\bar{\eta}a_1 + 2a_2). \tag{5.31}$$

By converting (5.30) back into a form involving exponentials it is relatively easy to obtain an analytical solution using the mathematical package MAPLE. The solution for ϕ_1 is

$$\begin{aligned}\phi_1 = {} & \frac{a_3(\sinh(2a_1\hat{\alpha}) + 2a_1\hat{\alpha})}{\cosh(a_1\hat{\alpha})} + \frac{a_4}{2\cosh(a_1\hat{\alpha})} \\ & - \frac{\left(2\lambda_1 a_1\hat{\alpha}\exp(a_1\hat{\alpha})\cosh(a_1\hat{\alpha}) + \frac{1}{2}\lambda_1\exp(2a_1\hat{\alpha}) - \frac{1}{4}\lambda_2 + \frac{3}{4}\lambda_1\right)}{2a_1^2\exp(a_1\hat{\alpha})(\cosh(2a_1\hat{\alpha}) + 1)},\end{aligned} \tag{5.32}$$

with a_3 and a_4 being integration constants. Finally, by making use of the boundary condition for ϕ_1 (5.19) and the limit condition (5.20) it is found that

$$a_3 = 0, \qquad a_4 = \frac{3\bar{\sigma}a_1 + 4\bar{\eta}a_1 - 2a_2}{2a_1}, \tag{5.33}$$

which gives the final form of the solution to be

$$\begin{aligned}\phi_1 = {} & \frac{\operatorname{sech}(a_1\hat{\alpha})}{16a_1^2}[5\lambda_1 - \lambda_2 - 8\lambda_1 a_1\hat{\alpha} - 2\lambda_1\exp(a_1\hat{\alpha})\operatorname{sech}(a_1\hat{\alpha}) \\ & - (3\lambda_1 - \lambda_2)\exp(-a_1\hat{\alpha})\operatorname{sech}(a_1\hat{\alpha})].\end{aligned} \tag{5.34}$$

By the results in (5.22), (5.23), (5.25), (5.27) and (5.34), the full inner solutions to order ϵ in the phase angle and to order ϵ^2 in the scaled potential are, respectively,

$$\phi = 2\tan^{-1}(\exp(a_1\hat{\alpha})) - \frac{\pi}{2} + \epsilon\frac{\operatorname{sech}(a_1\hat{\alpha})}{16a_1^2}[5\lambda_1 - \lambda_2 - 8\lambda_1 a_1\hat{\alpha} - 2\lambda_1\exp(a_1\hat{\alpha})\operatorname{sech}(a_1\hat{\alpha}) - (3\lambda_1 - \lambda_2)\exp(-a_1\hat{\alpha})\operatorname{sech}(a_1\hat{\alpha})], \tag{5.35}$$

and

$$\bar{\Psi} = \epsilon a_1\hat{\alpha} + \epsilon^2[a_2\hat{\alpha} - \bar{\eta}a_1\hat{\alpha} + \bar{\eta}\tanh(a_1\hat{\alpha})]. \tag{5.36}$$

5.3. The composite solution

Now that solutions have been obtained for the outer and inner regions of the wedge, all that remains is to combine them in some way to form a composite solution that is valid over the entire domain (in this case we only need a solution over half the domain due to symmetry arguments). This process is achieved using a standard matching method, where the outer solutions are expanded in terms of the inner variable, while the inner solutions are expanded in terms of the outer variable. These expansions are then truncated at a particular order and both are written in terms of the outer variable. By equating them, any undetermined constants can be found which then allows the full composite solution to be obtained.

Starting with the solutions for the scaled potential $\bar{\Psi}$ and by writing the outer solution (5.13) (which will be denoted by $\bar{\Psi}^o$) in terms of the inner variable $\hat{\alpha}$ (5.14) and expanding up to order ϵ^2 it is found that

$$\bar{\Psi}^o \approx (1 - 2b_0)\,\epsilon\hat{\alpha} + b_0 - 2b_1\epsilon^2\hat{\alpha} + b_1\epsilon + b_2\epsilon^2. \tag{5.37}$$

Returning to the original outer variable $\bar{\alpha}$ it is clear that

$$(\bar{\Psi}^o)^i = (1 - 2b_0)\bar{\alpha} + b_0 + \epsilon(b_1 - 2b_1\bar{\alpha}) + b_2\epsilon^2, \tag{5.38}$$

where the superscript i denotes that the outer solution has been expanded in terms of the inner variable. Similarly, by writing the inner solution (5.36) (denoted by $\bar{\Psi}^i$) in terms of the outer variable $\bar{\alpha}$ (5.14) and expanding up to order ϵ^2 gives

$$(\bar{\Psi}^i)^o = a_1\bar{\alpha} + (a_2\bar{\alpha} - \bar{\eta}a_1\bar{\alpha})\epsilon + \bar{\eta}\epsilon^2, \tag{5.39}$$

where the superscript o denotes that the inner solution has been expanded in terms of the outer variable. Now setting $(\bar{\Psi}^o)^i = (\bar{\Psi}^i)^o$ and comparing coefficients of powers of ϵ and of $\bar{\alpha}$ it is straightforward to show that the integration constants are given by

$$a_1 = 1, \qquad a_2 = \bar{\eta}, \qquad b_0 = 0, \qquad b_1 = 0, \qquad b_2 = \bar{\eta}. \tag{5.40}$$

The form of the final composite solution is given via [20, p 95]

$$\bar{\Psi} = \bar{\Psi}^o + \bar{\Psi}^i - (\bar{\Psi}^o)^i, \tag{5.41}$$

which, upon inserting (5.13), (5.14), (5.36), (5.38) and (5.40), yields the solution

$$\bar{\Psi} = \bar{\alpha} + \epsilon^2\left[\bar{\eta}\tanh\left(\frac{\bar{\alpha}}{\epsilon}\right) - 2\bar{\eta}\bar{\alpha}\right]. \tag{5.42}$$

The full solution for the phase angle ϕ can be found now that all the unknowns have been obtained. Clearly, from equation (5.12), $(\phi^o)^i = \frac{\pi}{2}$ and so the composite solution simplifies to

$$\phi = \phi^o + \phi^i - (\phi^o)^i = \phi^i. \tag{5.43}$$

Finally, from the scaling (5.14), the inner solution (5.35), the introduced parameters (5.31) and the evaluated constants of integration (5.40), the full solution can be written in the form

$$\phi = 2\tan^{-1}\left[\exp\left(\frac{\bar{\alpha}}{\epsilon}\right)\right] - \frac{\pi}{2} + \frac{1}{8}\operatorname{sech}\left(\frac{\bar{\alpha}}{\epsilon}\right)\left[(6\bar{\sigma}+4\bar{\eta})\,\epsilon - 4\bar{\sigma}\bar{\alpha}\right.$$
$$\left. - \bar{\sigma}\epsilon\exp\left(\frac{\bar{\alpha}}{\epsilon}\right)\operatorname{sech}\left(\frac{\bar{\alpha}}{\epsilon}\right) - (5\bar{\sigma}+4\bar{\eta})\,\epsilon\exp\left(-\frac{\bar{\alpha}}{\epsilon}\right)\operatorname{sech}\left(\frac{\bar{\alpha}}{\epsilon}\right)\right]. \tag{5.44}$$

In order to compare with the numerical work in Smith and Stewart [17], it is necessary to convert these solutions so that they are in terms of the original variables α and Ψ. From (2.17) it is seen that

$$\Psi = \left[\frac{\alpha}{\beta} + \epsilon^2\left(\bar{\eta}\tanh\left(\frac{\alpha}{\beta\epsilon}\right) - 2\bar{\eta}\frac{\alpha}{\beta}\right)\right]V_{\text{app}}, \tag{5.45}$$

and

$$\phi = 2\tan^{-1}\left[\exp\left(\frac{\alpha}{\beta\epsilon}\right)\right] - \frac{\pi}{2} + \frac{1}{8}\operatorname{sech}\left(\frac{\alpha}{\beta\epsilon}\right)\left[(6\bar{\sigma}+4\bar{\eta})\,\epsilon - 4\bar{\sigma}\frac{\alpha}{\beta} - \bar{\sigma}\epsilon\exp\left(\frac{\alpha}{\beta\epsilon}\right)\right.$$
$$\left.\times\operatorname{sech}\left(\frac{\alpha}{\beta\epsilon}\right) - (5\bar{\sigma}+4\bar{\eta})\,\epsilon\exp\left(-\frac{\alpha}{\beta\epsilon}\right)\operatorname{sech}\left(\frac{\alpha}{\beta\epsilon}\right)\right], \tag{5.46}$$

where $\epsilon = 1/U$, $\bar{\sigma} = \sigma/\epsilon$ and $\bar{\eta} = \eta/\epsilon$ (see (5.1)). Once again, it is more useful to investigate the behaviour of the electric field throughout the sample rather than the potential. Using equation (2.10), a calculation shows that the electric field is given by

$$\mathbf{E} = -\widehat{\boldsymbol{\alpha}}\frac{V_{\text{app}}}{r\beta}\left[1 + \bar{\eta}\epsilon\operatorname{sech}^2\left(\frac{\alpha}{\beta\epsilon}\right) - 2\bar{\eta}\epsilon^2\right], \tag{5.47}$$

and, by normalizing with respect to the critical field (see equation (3.16)), this allows the r-dependence to be eliminated to see that

$$\frac{E}{E_c} = \frac{V_{\text{app}}}{V_c}\left[1 + \bar{\eta}\epsilon\operatorname{sech}^2\left(\frac{\alpha}{\beta\epsilon}\right) - 2\bar{\eta}\epsilon^2\right]. \tag{5.48}$$

Figures 6 to 10 show how the director and field vary across the wedge for a variety of voltage ratios, permittivity values and elastic constants. The dashed curves are the solutions to the asymptotic expansions (5.46) and (5.48) and, for comparison, the numerical solutions obtained using the method outlined by Smith and Stewart [17] are given as solid curves. Unless otherwise noted in the figure captions, the data used are taken to be those in (4.25).

From figure 6 it is reassuring to observe the high degree of accuracy obtained by the asymptotic solutions for high voltage ratios. Even at twice the threshold value, the asymptotic solution agrees well with the numerical results. Although the asymptotic expansions are derived assuming σ and η to be of order ϵ, from figures 7–10 it is clear that, for physically realistic values for the parameters $\epsilon_{\|}$, B_1 and B_2, the approximations provide good fits to the numerical solutions.

6. Discussion

From previous work [7, 9, 10, 21, 22] it is already known that the SmC wedge geometry serves as an important tool for obtaining information regarding the material properties of liquid crystals. As a first approximation these articles assume that the field is uniform across the cell which, although accurate for magnetic fields, is not necessarily a realistic representation

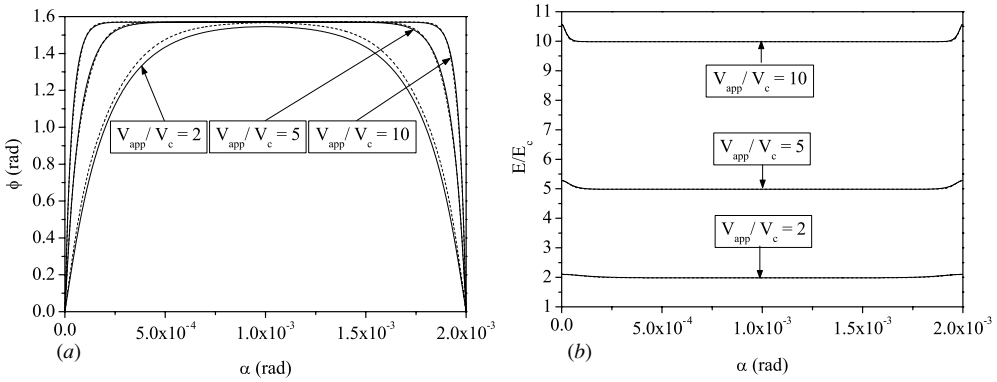

Figure 6. (*a*) Director behaviour and (*b*) field distortion across the SmC wedge for different applied voltage ratios, with the dashed and solid curves representing the asymptotic and numerical solutions, respectively. The parameter values are given by (4.25).

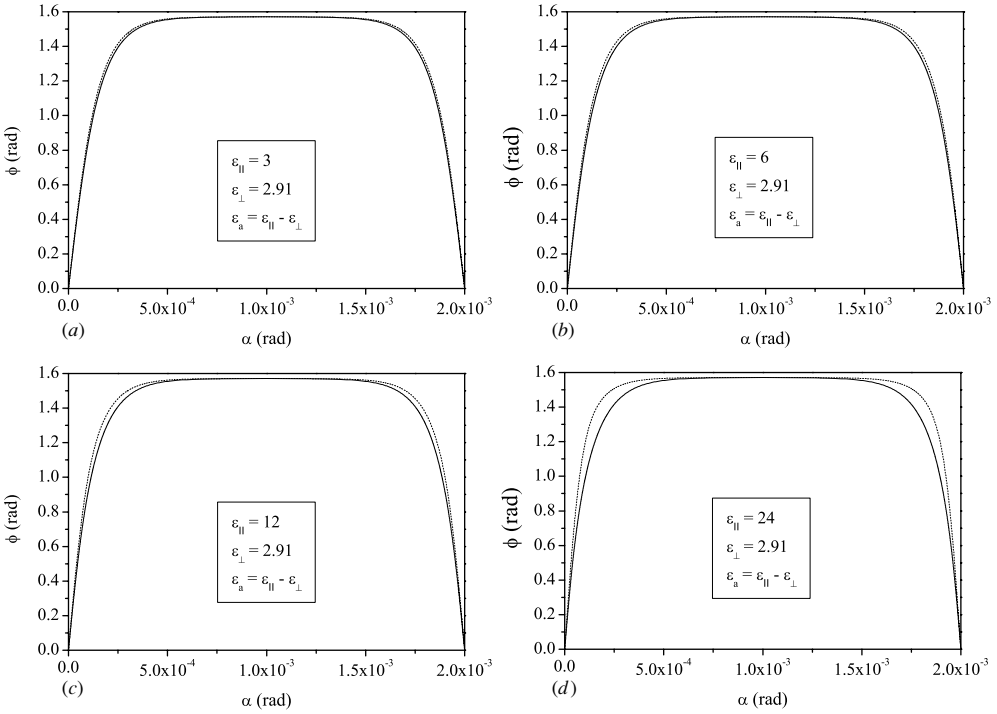

Figure 7. Director behaviour across the SmC wedge for different values of $\epsilon_{\|}$, with the dashed and solid curves representing the asymptotic and numerical solutions, respectively. Here, $V_{\rm app}/V_c = 3$ while the remaining parameters are given by (4.25) with the exception that $B_1 = B_2 = 5 \times 10^{-12}$N.

for electric fields. In order to provide a more accurate theoretical model to describe the orientation pattern of the director in such a cell, we have allowed for a two-way interaction between the material and an applied electric field. The analytical results obtained for various limiting regimes are supported by numerical calculations and the work is consistent with earlier research.

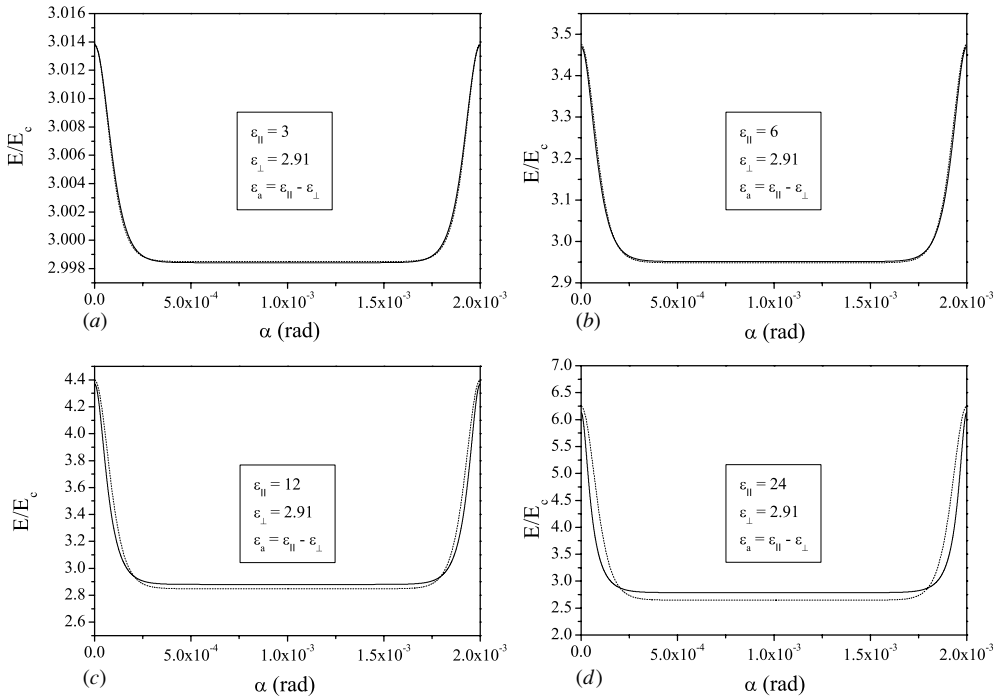

Figure 8. Field distortion across the SmC wedge for different values of $\epsilon_{\|}$ when $V_{\text{app}}/V_c = 3$, with the dashed and solid curves representing the asymptotic and numerical solutions, respectively. The remaining parameters are given by (4.25) with the exception that $B_1 = B_2 = 5 \times 10^{-12}$ N.

The current authors previously investigated some aspects of this problem [17] by obtaining a set of three coupled integral equations which were valid for any values of the material parameters and applied voltage. Unfortunately, their complexity forced the use of cumbersome numerical methods which, although sufficient to describe the behaviour, offered little information on the precise relationship between the director and field profiles and the material and geometry parameters. The method adopted in this paper is vastly more mathematically comprehensive and involves a rigorous analytical approach that culminates in explicit expressions for the director orientation and field behaviour at low and high field strengths (see equations (4.20), (4.23), (5.46) and (5.48)). Although only valid under certain conditions, these expressions provide immediate and clear insight into the static behaviour. Expressions such as these are not available when a numerical route is taken to the solution and to the authors' knowledge they are not to be found elsewhere in the literature. These explicit solutions, which display the influence of the material parameters upon the field behaviour, should be of great interest to anyone investigating post-threshold behaviour in the SmC wedge geometry and may prove valuable in obtaining additional information about the various material parameters.

From standard SmC continuum theory [2, 5–7], governing equations have been obtained and then solved using asymptotic methods which gave rise to informative solutions under several regimes. Under the assumption that the dielectric anisotropy is small, it has been found that the model reduces to that developed by Atkin and Stewart [9] and thereby highlights the area in which a uniform field approximation is valid. The region of most interest occurs when the applied voltage is just above the threshold (up to $V_{\text{app}}/V_c \approx 1.1$). Under this

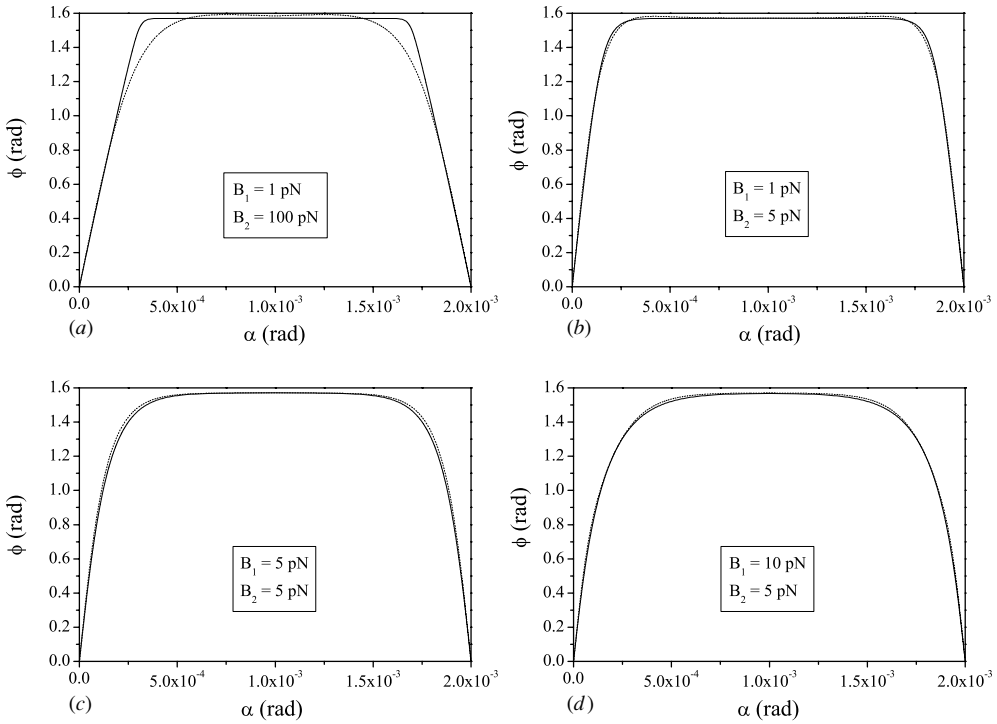

Figure 9. Director behaviour across the SmC wedge for different values of B_1 and B_2 when $V_{\text{app}}/V_c = 3$, with the dashed and solid curves representing the asymptotic and numerical solutions, respectively. The remaining parameters are given by (4.25) with the exception that $\epsilon_{\|} = 6$.

condition, the director orientation pattern obtained can vary significantly and depends upon the magnitude of the dielectric anisotropy. This variance in behaviour is caused entirely by the field being influenced by the material and is absent in the uniform field model which predicts that for a given value of V_{app}/V_c the director orientation is independent of the dielectric anisotropy. It should be remembered, of course, that the magnitude of the critical threshold is still dependent upon the dielectric anisotropy. Within this regime the director orientation takes on a standard half period sinusoidal solution (see equation (4.20)) with the magnitude being explicitly determined by the perturbation parameter and the combination of material and geometry parameters defined by λ (see equation (4.12)). Meanwhile, the electric field is perturbed around a constant solution via a full period cosine function (see equation (4.23)).

Further asymptotic expansions were derived and gave rise to expressions for the director and field behaviour at high voltages. It was found that these asymptotic solutions were valid for $V_{\text{app}}/V_c \gtrsim 2$ and were in good agreement with the numerical solutions. In order to make progress within this regime, conditions had to be imposed on the magnitudes of some of the material parameters (σ and η were assumed to be of order ϵ). However, it was found that these conditions were not that restrictive when supplying realistic data to the solutions. When considering voltages that are much greater than threshold it was found that the director orientation takes on a more complicated form (see equation (5.46)) involving a mixture of trigonometric and exponential terms which accurately model the flattening of the profile and steep director gradients near the boundaries. The corresponding field is modified from a

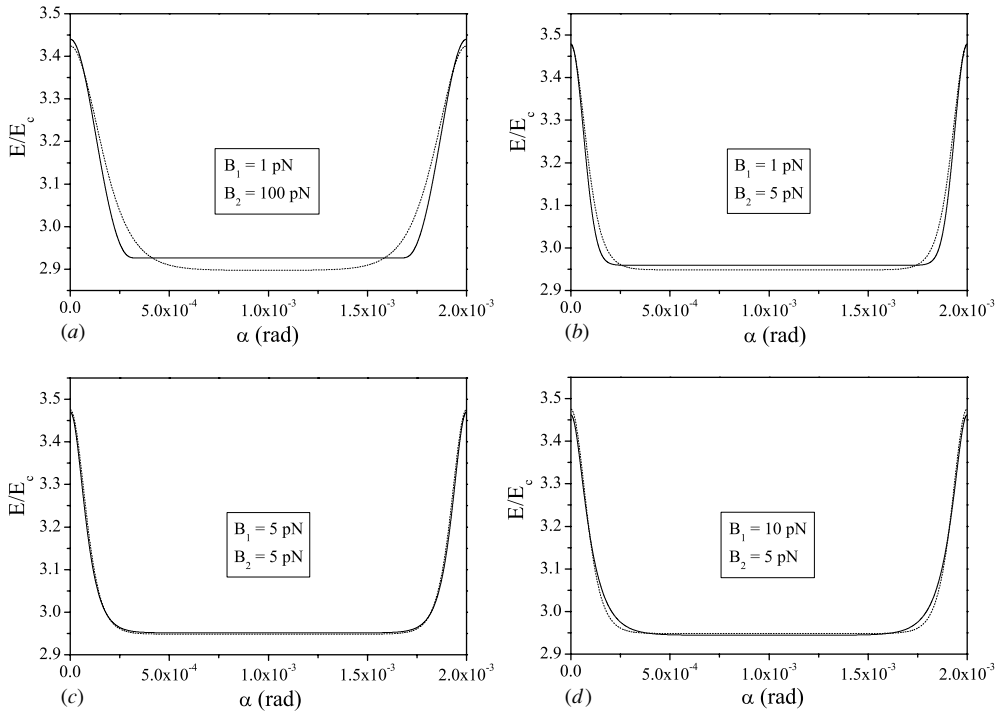

Figure 10. Field distortion across the SmC wedge for different values of B_1 and B_2 when $V_{\text{app}}/V_c = 3$, with the dashed and solid curves representing the asymptotic and numerical solutions, respectively. The remaining parameters are given by (4.25) with the exception that $\epsilon_{\|} = 6$.

constant solution via a hyperbolic secant function (see equation (5.48)), the amount of which is governed entirely by the perturbation parameter and $\bar{\eta}$.

In summary, we have used standard asymptotic methods to obtain analytical results for the Freedericksz transition in a wedge of SmC liquid crystal when the electric field exceeds the Freedericksz threshold. The influence of material parameters upon the derived asymptotic solutions has been investigated and revealed through the explicit forms for these solutions. The general results agree favourably with earlier exploratory numerical solutions.

Acknowledgment

AATS wishes to thank the UK EPSRC for funding made available to Strathclyde University.

References

[1] De Gennes P G and Prost J 1993 *The Physics of Liquid Crystals* 2nd edn (Oxford: Clarendon)
[2] Stewart I W 2004 *The Static and Dynamic Continuum Theory of Liquid Crystals* (London: Taylor and Francis)
[3] Rapini A 1972 *J. Phys. (Paris)* **33** 237
[4] Orsay Group 1971 *Solid State Commun.* **9** 653
[5] Leslie F M, Stewart I W and Nakagawa M 1991 *Mol. Cryst. Liq. Cryst.* **198** 443
[6] Leslie F M, Stewart I W, Carlsson T and Nakagawa M 1991 *Contin. Mech. Thermodyn.* **3** 237
[7] Carlsson T, Stewart I W and Leslie F M 1991 *Liq. Cryst.* **9** 661
[8] Atkin R J and Stewart I W 1994 *Q. J. Mech. Appl. Math.* **47** 231

[9] Atkin R J and Stewart I W 1997 *Liq. Cryst.* **22** 585
[10] Atkin R J and Stewart I W 1997 *Eur. J. Appl. Math.* **8** 253
[11] Kedney P J and Stewart I W 1994 *Z. Angew. Math. Phys.* **45** 882
[12] Barratt P J and Duffy B R 1997 *Liq. Cryst.* **23** 525
[13] Kidd J E, Stewart I W and Constanda C 2001 *IMA J. Appl. Math.* **66** 387
[14] Pelzl G, Schiller P and Demus D 1987 *Liq. Cryst.* **2** 131
[15] Deuling H J 1972 *Mol. Cryst. Liq. Cryst.* **19** 123
[16] Welford K R and Sambles J R 1987 *Mol. Cryst. Liq. Cryst.* **147** 25
[17] Smith A A T and Stewart I W 2004 *Mol. Cryst. Liq. Cryst.* **413** 251
[18] Schiller P 1989 *Liq. Cryst.* **4** 69
[19] Self R H, Please C P and Sluckin T J 2002 *Eur. J. Appl. Math.* **13** 1
[20] Van Dyke M 1964 *Perturbation Methods in Fluid Mechanics* (New York: Academic)
[21] Stewart I W 1999 *Phys. Rev.* E **60** 1888
[22] Findon A and Gleeson H F 2002 *Ferroelectrics* **277** 35
[23] Oseen C W 1933 *Trans. Faraday Soc.* **29** 883
[24] Jones J C and Raynes E P 1992 *Liq. Cryst.* **11** 199
[25] Lorrain P, Corson D R and Lorrain F 1988 *Electromagnetic Fields and Waves* 3rd edn (New York: Freeman)
[26] Smirnov V I 1964 *A Course of Higher Mathematics (Integral Equations and Partial Differential Equations* vol 4*)* (Oxford: Pergamon)
[27] Gray G W and Goodby J W 1984 *Smectic Liquid Crystals: Textures and Structures* (Glasgow: Leonard Hill)
[28] Dunmur D A, Fukuda A and Luckhurst G R (ed) 2001 *Physical Properties of Liquid Crystals: Nematics (EMIS Datareviews Series* vol 25*)* (London: The Institution of Electrical Engineers (INSPEC))
[29] Brown C V, Dunn P E and Jones J C 1997 *Eur. J. Appl. Math.* **8** 281